 FDMP, vol.5, no.3, pp.283-295, 2009

Coupling of Lattice Boltzmann Equation and Finite Volume Method to Simulate Heat Transfer in a Square Cavity

Ahmed Mezrhab[1] **and Hassan Naji**[2]

Abstract: The objective of this paper is to assess the effectiveness of the coupled Lattice Boltzmann Equation (LBE) and finite volume method strategy for the simulation of the interaction between thermal radiation and laminar natural convection in a differentially heated square cavity. The vertical walls of the cavity are adiabatic, while its top and bottom walls are cold and hot, respectively. The air velocity is determined by the lattice Boltzmann equation and the energy equation is discretized by using a finite volume method. The resulting systems of discretized equations have been solved by an iterative procedure based on a preconditioned conjugate gradient method. Only the surface radiation is taken into account and the walls of the enclosure are assumed to be diffuse-grey. The achieved simulations have shown that the coupling between the lattice Boltzmann equation and the finite volume method gives excellent results. It was also observed that the surface radiation standardizes the temperature inside the cavity and causes a considerable increase of the heat transfer.

Keywords: Lattice Boltzmann Equation; Hybrid scheme; Finite volume; Natural convection, Radiative transfer.

Nomenclature

A_i	i^{th} radiative surface
F_{ij}	view factor between A_i and A_j
g	gravity acceleration, ms^{-2}
k	thermal conductivity, $Wm^{-1}K^{-1}$
L	cavity length, m

[1] Corresponding author. Faculté des Sciences, Département de Physique, Laboratoire de Mécanique & Energétique, 60000 Oujda, Maroc. Tel.: +212-36 50 06 01/02; fax: +212-36 50 06 03; E-mail address: amezrhab@yahoo.fr; mezrhab@fso.ump.ma.

[2] USTL/Polytech'lille/LML UMR 8107 CNRS, Département de Mécanique, F-59655 Villeneuve, d'Ascq Cedex, France.

Nu	Average Nusselt number
N_r	radiation number, $\sigma T_h^4/(k\Delta T/L)$
Pr	Prandtl number, ν/α
q_r	net radiative flux density, Wm^{-2}
Q_r	dimensionless net radiative flux density, $q_r/\sigma T_h^4$
Ra	Rayleigh number, $g\beta(T_h-T_c)L^3/\nu\alpha$
R_i	Radiosity of radiative surface A_i
T	temperature, K
T_0	Average temperature, $(T_h+T_c)/2$, K
u,w	velocity component along x, y, ms^{-1}
U,W	dimensionless velocity components along x, y. $U=uL/\alpha$, $W=wL/\alpha$
x,y	Cartesian coordinates, m
X,Y	dimensionless Cartesian coordinates, $X=x/L$, $Y=y/L$

Greek symbol

ε_i	emissivity of radiative surface A_i
α	thermal diffusivity of the fluid, m^2s^{-1}
β	volumetric expansion coefficient, K^{-1}
ΔT	maximal difference temperature, (T_h-T_c), K
ν	kinematic viscosity of the fluid, m^2s^{-1}
θ	dimensionless temperature, $(T-T_0)/(T_h-T_c)$
Θ	dimensionless temperature, T/T_h
σ	Stefan-Boltzmann constant, $Wm^{-2}K^{-4}$

Subscripts

h	hot
c	cold

1 Introduction

Natural convection in two-dimensional vertical rectangular cavities is one of the standard fluid flow and heat transfer cases used for the validation of computational

fluid dynamics (CFD) codes and their development. This interest is due to their industrial applications in a variety of engineering problems such as solar, thermal habitat and the cooling of electronic components. Usually, the numerical methods used for these simulations are based on the spatial and temporal discretization of macroscopic evolution equations. However, their solutions can be very complex when dealing with problems where the geometry is complex or in presence of several phases of a fluid or more fluids. That is why a different approach called "Lattice Cellular Gas Automata" has been developed (see Frisch et al (1986)). This method is at the origin of the commonly known the Lattice Boltzmann Equation (LBE) which has emerged as a powerful alternative tool for the solution of fluid flows. Using velocity-space truncation of the Boltzmann equation from the kinetic theory of gases, the LBE methods lead to linear, constant coefficient hyperbolic systems with non-linear source terms. Its goal is to model the flow of a fluid at the microscopic level in terms of local interactions between the particles. Unlike traditional numerical methods which solve the macroscopic variables such as velocity and density directly, these variables are obtained in LBE by moment integrations of the particle distribution function. This method has many advantages: it is easier and intuitive to treat particular conditions such as the presence of obstacles or the multiphase flow. From a computational viewpoint, the notable advantages of this approach are its intrinsic parallelism of algorithm, simplicity of programming, and ease of incorporating microscopic interactions. It has been successfully used in many kinds of complex flows such as single component hydrodynamics, multiphase and multi-component fluids, magneto-hydrodynamics, reaction-diffusion systems, flows through porous media, turbulent flow (Chen and Doolen (1998); Mezrhab et al (2004, 2008); Semma et al (2007, 2008)). Detailed theoretical analysis has placed this approach on a solid foundation, and a large number of numerical validations have been carried out to assess its accuracy, especially in problems with mass and momentum conservation.

The main objective of this work is to assess the efficiency of the numerical coupling between the LBE in its refined multi-relaxation approach (d'Humières (1992)) and finite volume method in order to obtain the velocity and temperature fields. This approach is applied to investigate numerically the steady combined laminar natural convection and surface radiation heat transfer in a two-dimensional enclosure heated from below for various Rayleigh numbers at a fixed ΔT or L using air as the working fluid.

The remainder of this paper is organized as follows. In the next section, the mathematical and numerical formulations of the problem are described. The implementation details and the computed results are reported and discussed in Section 3. Finally, the major conclusions based on our numerical study are drawn in Section

4.

2 Mathematical formulation and numerical procedure

The geometry studied is presented in Figure 1. The sidewalls are adiabatic; the top horizontal wall is maintained at a cold temperature T_c, while the bottom horizontal wall is brought to a hot temperature T_h. The flow is assumed incompressible, laminar, steady and two-dimensional. The Boussinesq approximation is adopted in order to simplify the analysis. The considered fluid is the air and its physical properties are supposed to be constant at the average temperature T_0, except its density. The air is assumed as perfectly transparent to thermal radiation and thus, only solid surfaces contribute to the radiation exchange and are assumed to be diffuse-gray.

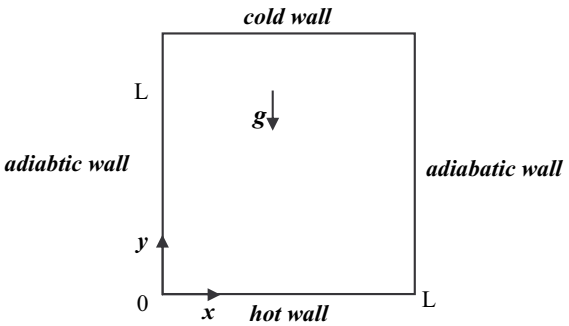

Figure 1: Schematic view of the square cavity.

2.1 Multiple Relaxation Time Lattice Boltzmann Equation (MRT-LBE)

The Lattice Boltzmann Equation (LBE) is a numerical scheme evolved from the Lattice Gas Model (LGM) in order to overcome the difficulties encountered with the LGM (Frisch et al (1986)). In LBE, the fluid field is discretized by a group of microscopic particles. The density distributions of these particles perform two types of motions: collision and streaming. In what follows, we use the $D2Q9$ model (see Figure 2) on a square lattice with lattice spacing $\delta x = \delta y$ (where D refers to space dimensions and Q to the number of particles at a computational node). Each node comprises three kinds of particles, rest particles that reside in the nodes of the lattice, particles that move along the coordinate directions and particles that move along diagonal directions.

The simplest lattice Boltzmann equation (LBE) is the lattice Bhatnagar-Gross-Krook (BGK) equation, based on a single-relaxation-time (SRT) approximation

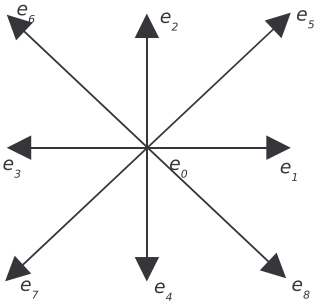

Figure 2: The structure of the lattice cell in D2Q9 model for LBE.

(see Bhatnagar (1954)). Due to its extreme simplicity, the lattice BGK equation has become the most popular lattice Boltzmann model. However, this simplicity comes at the expense of numerical instability (Lallemand and Luo (2000)) and inaccuracy in implementing boundary conditions (Ginzburg and d'Humières (2003)). These deficiencies in the BGK models can be overcome with the use of multiple relaxation-time (MRT) model introduced by d'Humières et al (2002). It has been clearly demonstrated that the LBE models with MRT collision operators have inherent advantages over their BGK counterparts (see Bhatnagar (1954); Lallemand and Luo (2000)). The MRT lattice Boltzmann equation (also referred to as the generalized lattice Boltzmann equation (GLBE) or the moment method) overcomes some obvious defects of the BGK model, such as fixed Prandtl number (Pr = 1 for the BGK model) and fixed ratio between the kinematic and bulk viscosities). The MRT-LBE models are much more stable than the BGK, since the different relaxation times can be individually tuned to achieve "optimal" stability (Lallemand and Luo (2000)).

For a MRT-LBE model with 9 velocities, a set of velocity distribution functions $f_i(r_j,t_n)$, $i \in \{0,\ldots,8\}$ is defined on each node r_j of the lattice and for time t_n. The evolution equation for the MRT-LBE of 9 velocities on a 2-dimensional lattice $r_j \in (\delta_x \mathrm{Z})^2$ with discrete time $t_n \in \delta_t \mathrm{N} = \delta_t \{0,1,2,\ldots\}$ is:

$$\mathbf{f}(\mathbf{r}_j + \mathbf{e}_i\delta_t, t_n + \delta_t) - \mathbf{f}(\mathbf{r}_j, t_n) = -M^{-1}S(\mathbf{m}(\mathbf{r}_j,t_n) - \mathbf{m}^{eq}(\mathbf{r}_j,t_n)) \tag{1}$$

where $\mathbf{f}(\mathbf{r},t)$, $\mathbf{m}(\mathbf{r},t)$ and $\mathbf{m}^{eq}(\mathbf{r},t)$ are 9-dimensional vectors for the distribution functions, the moments, and the equilibria of moments, respectively, e.g., $\mathbf{f} = (f_0,f_1,...,f_8)^T \in \mathrm{V}\left(=\mathrm{R}^9\right)$, and $\mathbf{m} = (m_0,m_1,...,m_8)^T \in \mathrm{M}\left(=\mathrm{R}^9\right)$, T being the

transport operator. M is the transformation matrix such that $\mathbf{m} = M\mathbf{f}$ and $\mathbf{f} = M^{-1}\mathbf{m}$ and S is the relaxation matrix in the moment space M. Explicitly, matrices M and S of the incompressible lattice Boltzmann model can be written as, respectively:

$$M = \begin{pmatrix} 1 & 1 & 1 & 1 & 1 & 1 & 1 & 1 & 1 \\ -4 & -1 & -1 & -1 & -1 & 2 & 2 & 2 & 2 \\ 4 & -2 & -2 & -2 & -2 & 1 & 1 & 1 & 1 \\ 0 & 1 & 0 & -1 & 0 & 1 & -1 & -1 & 1 \\ 0 & -2 & 0 & 2 & 0 & 1 & -1 & -1 & 1 \\ 0 & 0 & 1 & 0 & -1 & 1 & 1 & -1 & -1 \\ 0 & 0 & -2 & 0 & 2 & 1 & 1 & -1 & -1 \\ 0 & 1 & -1 & 1 & -1 & 0 & 0 & 0 & 0 \\ 0 & 0 & 0 & 0 & 0 & 1 & -1 & 1 & -1 \end{pmatrix} \tag{2}$$

and

$$S = diag(0, s_1, s_2, 0, s_4, 0, s_6, s_7, s_8) \tag{3}$$

In the $D2Q9$ model, the discrete velocity set is:

$$e_i = \begin{cases} (0,0), & i = 0 \\ \left(\cos\left[(i-1)\frac{\pi}{2}\right], \sin\left[(i-1)\frac{\pi}{2}\right]\right) c, & 1 \le i \le 4 \\ \sqrt{2}c\left(\cos\left[(2i-9)\frac{\pi}{4}\right], \sin\left[(2i-9)\frac{\pi}{4}\right]\right), & 5 \le i \le 8 \end{cases} \tag{4}$$

where $c = \delta_x/\delta_t$ is the particle velocity and δ_x and δ_t are the lattice grid spacing and time step, respectively. From here on, we shall use the units of $\delta_x = \delta_t = 1$ such that all the relevant quantities correspond are dimensionless.

The nine components of the moment vector $\mathbf{m}$ are arranged in the following order: $m_0 = \rho$ is the fluid density, $m_1 = e$ is related to the energy, $m_2 = \varepsilon$ is related to the energy square, $m_{3,5} = j_{x,y}$ are components of the momentum $\mathbf{J} = (j_x, j_y)$, $m_{4,6} = q_{x,y}$ are related to components of the energy flux and $m_{7,8} = p_{xx,xy}$ are related to the components of the symmetric and traceless strain rate tensor. These nine moments are separated into two groups: (ρ, m_3, m_5) are the conserved moments which are locally conserved in the collision process; $(m_1, m_2, m_4, m_6, m_7, m_8)$ are the non-conserved moments and they are calculated from the relaxation equations:

$$m_j^{ac} = m_j^{bc} + s_j(m_j^{eq} - m_j^{bc}) \tag{5}$$

where m_j^{ac} is the moment after collision, m_j^{bc} is the moment before collision (the post-collision value), s_j are the relaxation rates which are the diagonal elements of the matrix S and m_j^{eq} are the corresponding equilibrium moments. Note that the

collision rates s_0, s_3 and s_5 are not relevant, since they are related to the conserved moments. In order to obtain a consistant dynamics viscosity, relaxation rates s_7 and s_8 have to be equal $s_7 = s_8$. The other relaxation rates have no physical meaning for incompressible flows and for stability reasons, they can be freely chosen in the range $0 < s_i < 2$.

In the lattice units of $\delta_x = \delta_t = 1$, the speed of sound is $c_s = 1/\sqrt{3}$ and the kinematic viscosity ν is given by:

$$\nu = c_s^2 \delta_t \left(\frac{1}{s_7} - \frac{1}{2} \right) = c_s^2 \delta_t \left(\frac{1}{s_8} - \frac{1}{2} \right) \tag{6}$$

The equilibrium values of the non-conserved moments $\mathbf{m}^{eq}$ are chosen to be:

$$\begin{aligned} e^{eq} &= -2\rho + 3(j_x^2 + j_y^2) \\ \varepsilon^{eq} &= \rho - 3(j_x^2 + j_y^2)/\rho_0 \\ q_x^{eq} &= -j_x \\ q_y^{eq} &= -j_y \\ p_{xx}^{eq} &= (j_x^2 - j_y^2)/\rho_0 \\ p_{xy}^{eq} &= j_x j_y / \rho_0 \end{aligned} \tag{7}$$

The constant ρ_0 is the mean density in the system and is usually set to be unity in simulations.

The macroscopic fluid variables, density ρ and velocity $\mathbf{u}$, are obtained from the moments of the distribution functions as follows:

$$\rho = \sum_{i=0}^{8} f_i \tag{8}$$

$$\mathbf{J}(j_x, j_y) = \rho \mathbf{u} = \sum_i f_i \mathbf{e}_i \tag{9}$$

where $\mathbf{u}(u,w)$ is the air velocity vector.

It should be noted that the presence of the force density $g\beta\Delta T\theta(\mathbf{r},t)$ modifies the conservation of the vertical velocity in the stage of collision, which translates into:

$$w^{ac} = w^{bc} + g\beta\Delta T\theta(\mathbf{r},t) \tag{10}$$

where w^{ac} et w^{bc} represent the vertical velocity respectively before and after the collision.

The dynamic boundary conditions on the walls of the cavity are imposed by the so-called bounce-back rule, which makes it possible to obtain $u = w = 0$ at all walls of the cavity (Mezrhab et al (2004)).

This method has been well explained in our previous works and for more details, the reader can to refer to the papers (Mezrhab et al (2004, 2008)).

2.2 Fields temperature

The energy equation is given by:

$$U\frac{\partial\theta}{\partial X}+W\frac{\partial\theta}{\partial Y}=\left(\frac{\partial^2\theta}{\partial X^2}+\frac{\partial^2\theta}{\partial Y^2}\right) \tag{11}$$

The thermal boundary conditions used are:

$\theta = 0.5$ for $Y = 0$ and $0 \leq X \leq 1$

$\theta = -0.5$ for $Y = 1$ and $0 \leq X \leq 1$

At the adiabatic walls: $X = 0$ or 1 and $0 \leq Y \leq 1$

$$\frac{\partial\theta}{\partial Y}-N_rQ_r=0 \tag{12}$$

In order to ensure the grid-independence solutions, a series of trial calculation were conducted for different grid distributions, and the optimal mesh that allows for a good compromise (accuracy / computing time) is 101×101.

The energy equation (Eq. 11) was discretized by a finite volume method with discretization scheme centred in terms of transport. The resulting systems of discretized equations were solved by means of an iterative procedure based on a preconditioned conjugate gradient method

In order to discretize the equation (12), the surfaces of solid radiative forming the cavity were discretized in a number N of radiative surfaces. N is the total number of radiative surfaces, which is equal to the total number of volumes of interfaces between solid and fluid controls. Therefore, the dimensionless density of the radiative flux $Q_{r,i}$ lost by the surface A_i is given by:

$$Q_{r,i}=R_i-\sum_{j=1}^{N}R_jF_{i-j} \tag{13}$$

In addition, the dimensionless radiosity is obtained by solving the system:

$$\sum_{j=1}^{N}\left(\delta_{ij}-(1-\varepsilon_i)F_{i-j}\right)R_j=\varepsilon_i\Theta_i^4 \tag{14}$$

where δ_{ij} is the Kronecker symbol.

For the combined radiation and convection problem, the surface temperatures on the insulated wall were calculated from the non-linear heat balance (Eq. 12) by using an inner iterative procedure at every time step for the energy equations. The surface temperatures were updated from the solution of the energy equation by under-relaxing the boundary evaluation of temperature. At each inner iteration, the linear system of equations for the radiosities (Eq. 14) was solved by a direct method (Gauss elimination). The grid was constructed such that the boundaries of physical domain coincide with the velocity grid lines. The points for temperature were placed at the center of the scalar volumes. At the fluid-adiabatic wall interfaces, the control volume faces were also arranged so that a control volume face coincided with an interface. This grid distribution was chosen to ensure the interface energy balance. To avoid a check-board pressure and velocity fields, staggered grids were used for the U and W-velocity components in the X and Y-directions respectively.

Table 1: Average Nusselt-number comparisons for $Pr = 0.71$ and $\varepsilon = 0$

Ra	10^3	10^4	10^5	10^6	10^7
Present	1.118	2.242	4.524	8.824	16.490
De Vahl Davis (1983); Le Quéré (1991)	1.118	2.243	4.523	8.826	16.510

Since the radiative properties of the solid surfaces of the plate and of the insulated wall vary from point to point, each of the surfaces was divided into finite number of zones on which the four basic assumptions of the simplified zone analysis was assumed valid. The mesh used to solve the differential equations determined the number of zones retained. Therefore, the zoning was not uniform and the area of each zone varied according to the stretching function and number of grid points used. For N control volume faces, this results in $N(N-1)/2$ view factors to be calculated and in a linear system of N equations for the radiosities. The view factors were determined by using a boundary element approximation to fit the surfaces and on a Monte Carlo method for the numerical integrations (Mezrhab and Bouzidi (2005)).

To characterize heat transfers, the average Nusselt number at the hot wall is expressed as:

$$Nu = \int_0^1 \left(-\left.\frac{\partial \theta}{\partial Y}\right|_{X,Y=0} + N_r Q_r (X, Y=0) \right) dX \tag{15}$$

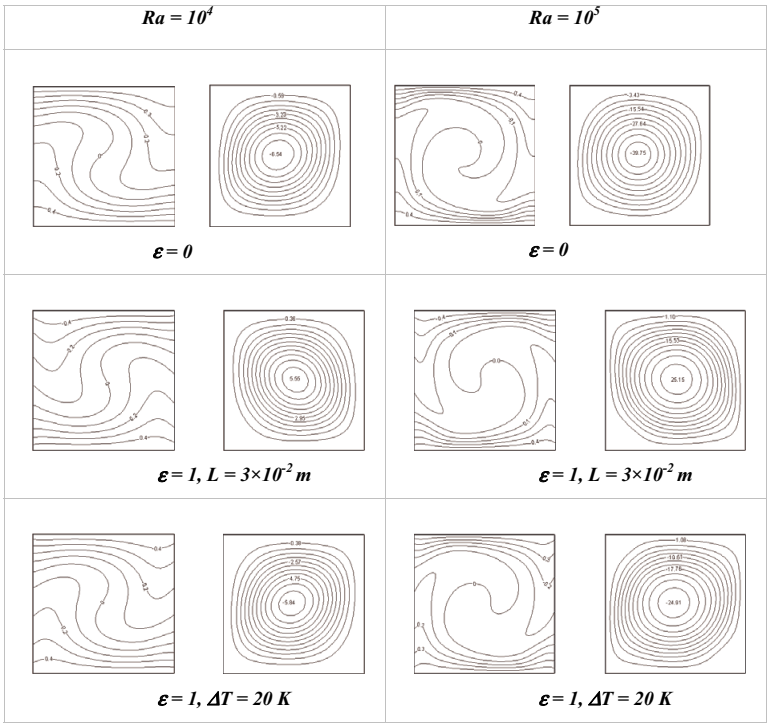

Figure 3: Isotherms and streamlines in absence ($\varepsilon = 0$) and in presence ($\varepsilon = 1$) of the radiation exchange for $Ra = 10^4$ and 10^5.

3 Examples of simulations

The code has been exercised intensively on benchmark problems to check its validity. We present in the table 1 the comparison between some results obtained in natural convection using our house code with those reported in references [13-14]. The case considered is that of a square differentially heated. The horizontal end walls are perfectly insulated whereas the two vertical walls are maintained at two different temperatures T_h and T_c respectively.

When the radiation exchange is taken into account, our code has been validated with the numerical results published previously by different authors, and the agreement between the present and previous results was very good in reference Mezrhab et al (2007). For this reason and for brevity we do not repeat here. Based on the above studies, it was concluded that the code could be correctly applied to the problem under consideration.

In pure natural convection, each configuration depends at least two dimensionless

parameters (Pr, Ra). Taking into account the surface radiation requires the knowledge of four other parameters (T_0, ΔT, L, ε). Pr and T_0 are fixed to 0.71 and 300 K, respectively. The thermophysical properties of the air at 300 Kshows that the term $(g\beta/\nu\alpha)$ is approximately equal to $9\times10^7\ m^{-3}K^{-1}$; so the Rayleigh number varying from 10^3 to 10^6, is only function of ΔT and L. The emissivity ε of radiative surfaces is chosen equal to 0 in pure natural convection and equal to 1 in presence of the radiation exchange. In this paper, two cases were considered: in the first case, we have fixed ΔT to 20 K and we have calculated L for each value of Ra, and in the second case, we have fixed L to $3\times10^{-2}m$ and ΔT was calculated for each value of Ra. The radiation number Nr is determined as function of Ra, ΔT and L according to its expression mentioned in nomenclature.

Figure 3 presents isotherms and streamlines either in presence or in absence of the radiation exchange for two Rayleigh numbers 10^4 and 10^5. In the case of the cavity heated by the bottom horizontal wall, it has been shown in the past, the presence of multiple solutions in steady state (see Hasnaoui et al (1992)). The Rayleigh numbers considered in this study produce mono cellular with possible rotations in the clockwise and counter-clockwise directions.

In presence of the radiation exchange, ($\varepsilon = 1$), the temperature gradients near the vertical walls give an indication of the importance of radiative flux. The streamlines show that the radiation exchange reduces considerably the circulation in the cavity. In fact, the radiation exchange reduces the temperature difference between the adiabatic walls and therefore decreases the air velocity near these walls.

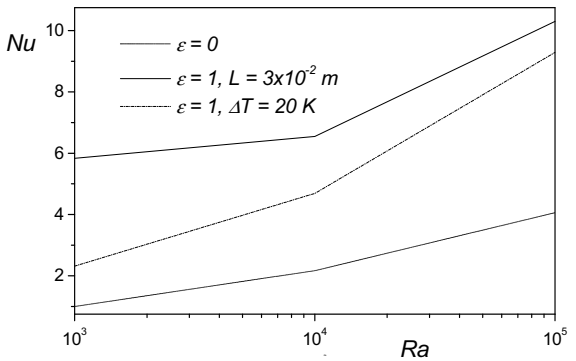

Figure 4: Variation of average Nusselt number as function of Ra.

The average Nusselt number is presented in figure 4. It is observed that the average Nusselt number increases under the effect of the buoyancy force (increase of Ra) and the surface radiation. This can be explained by the fact that the contribution of

the radiative exchange to the average Nusselt is controlled by the productN_rQ_r, as indicated in Eq. 15. As can be seen, the average Nusselt number is proportional to the product N_rQ_r, which increases with increasing Ra, whatsoever when taking of ΔT or L.

4 Conclusion

Numerical resolution of natural convection coupled with radiative heat transfer is carried out in a square cavity, whose the sidewalls are adiabatic, while the bottom and the top horizontal walls are maintained at two different temperatures T_h and T_c, respectively. The methodology used is a hybrid numerical scheme based on the lattice Boltzmann equation combined with the finite volume method. Within the investigated parameters range, the following conclusions can be drawn:

1). The combination of lattice Boltzmann equation and the finite volume method is very successful;

2). The surface radiation homogenized the temperature inside the cavity by reducing the difference in temperature between the adiabatic walls. It also reduces the air circulation in the cavity;

3). The surface radiation increases the heat transfer in the cavity.

References

Bhatnagar, P.L.; Gross, E.P.; Krook, M. (1954): A model for collision processes in gases. I. Small amplitude processes in charged and neutral one-component systems. *Phys. Rev.*, 94, 511-525.

Chen, S.Y.; Doolen, G.D. (1998): Lattice Boltzmann method for fluid flows, *Annual Review of Fluid Mechanics*, vol. 30, pp. 329-364.

De Vahl Davis, G. (1983): Natural convection in air in a square cavity: A Bench Mark Numerical Solution, *Int. J. Num. Meth. Fluids*, vol. 3, pp. 249-264.

d'Humières, D. (1992): Generalized lattice-Boltzmann equations, in B.D. Shizgal, D.P. Weaver (Eds.), Rarefied Gas Dynamics: Theory and Simulations, *Prog. Astronaut. Aeronaut.*, 159, AIAA, Washington, DC, 450-458.

d'Humières, D.; Ginzburg, I.; Krafczyk, M.; Lallemand, P.; Luo, L.S. (2002): Multiple-relaxation-time lattice Boltzmann models in three-dimensions. *Philos Trans R Soc London A*, vol. 360, pp. 437-451.

Frisch, U.; Hasslacher, B.; Pomeau, Y. (1986): Lattice-gas automata for the Navier–Stokes equation. *Phys Rev Lett*, 56, 1505-1508.

Ginzburg, I.; d'Humières, D. (2003): Multireflection boundary conditions for lattice Boltzmann models. *Phys Rev E*, 68, 066614.

Hasnaoui, M.; Bilgen, E.; Vasseur, P. (1992): Natural convection Heat Transfer in rectangular cavities partially heated from below, *J. Thermophys. Heat Transfer*, vol. 6, no. 2, pp. 255-264.

Lallemand, P.; Luo, L.S. (2000): Theory of the lattice Boltzmann method: Dispersion, dissipation, isotropy, Galilean invariance, and stability. *Phys Rev E*, vol. 61, pp. 6546-6562.

Le Quéré, P. (1991): Accurate solutions to the square thermally driven cavity at high Rayleigh number, *Computers & Fluids*, vol. 20, no. 1, pp. 29-41.

Mezrhab, A.; Bouzidi, M.; Lallemand, P. (2004): Hybrid lattice-Boltzmann finite-difference simulation of convective flows, *Computers & Fluids*, vol. 33, pp. 623-641.

Mezrhab, A.; Bouzidi, M. (2005): Computation of view factors for surfaces of complex shape including screening effects and using a boundary element, *Engineering Computations: International Journal for Computer-Aided Engineering and software*, vol. 22, no 2, pp. 132-148.

Mezrhab, A.; Jami, M.; Bouzidi, M.; Lallemand, P. (2007): Analysis of radiation–natural convection in a divided enclosure using the lattice Boltzmann method, *Computers & Fluids*, Vol. 36, no. 2, pp. 423-434.

Mezrhab, A.; Moussaoui, M.A.; Naji, H. (2008): Lattice Boltzmann simulation of surface radiation and natural convection in a square cavity with an inner cylinder, *J. Phys. D: Appl. Phys.*, vol. 41, 551-5517.

Semma, E.; El Ganaoui, M.; Bennacer, R. (2007): Lattice Boltzmann method for melting/solidification problems, *Comptes Rendus Mécanique*, 335 5-6 295-303.

Semma, E.; El Ganaoui, M.; Bennacer, R.; Mohamad, A.A. (2008): Investigation of flows in solidification by using the lattice Boltzmann method, *International Journal of Thermal Sciences*, vol. 47, no. 3, pp. 201-208.